

## ***Supporting Information***

# **Structure and stereospecificity of the dehydratase domain from the terminal module of the rifamycin polyketide synthase**

Darren Gay,<sup>a,†</sup> Young-Ok You,<sup>b,†</sup> Adrian T. Keatinge-Clay<sup>a,\*</sup>, & David E. Cane,<sup>b,\*</sup>

<sup>a</sup>Department of Chemistry and Biochemistry, the University of Texas at Austin, 1 University Station  
A5300, Austin, TX 78712-0165

<sup>b</sup>Department of Chemistry, Brown University, Box H, Providence RI 02912-9108, USA

\*To whom correspondence should be addressed: david\_cane@brown.edu; adriankc@utexas.edu

†These authors contributed equally to this work.

## ***SI Table of Contents***

<b>Figure S1.</b> Polyketides with <i>cis</i> double bonds	S4
<b>Figure S2.</b> Dehydration of (2 <i>R</i> ,3 <i>S</i> )- and (2 <i>R</i> ,3 <i>R</i> )-2-methyl-3-hydroxyacyl thioesters	S4
<b>Domain boundaries and design of recombinant RifDH10 and RifACP10</b>	S5
1. <b>Figure S3.</b> Rifamycin PKS partial module 9 and module 10	S5
2. <b>Figure S4.</b> RifDH10 amino acid sequence	S6
3. <b>Figure S5.</b> RifACP10 amino acid sequence	S6
<b>Figure S6.</b> SDS-PAGE of recombinant RifDH10-KR10, RifDH10 and RifACP10-NusA	S7
<b>Incubations of incubation of (2<i>RS</i>)-2-methyl-3-ketopentanoyl-RifACP10-NusA</b>	
1. <b>Figure S7.</b> Chiral GC-MS analysis of the incubation of (2 <i>RS</i> )-2-methyl-3-ketopentanoyl-RifACP10-NusA with RifKR7 in the absence of RifDH10	S8
2. <b>Figure S8.</b> Chiral GC-MS analysis of the incubation of (2 <i>RS</i> )-2-methyl-3-ketopentanoyl-RifACP10-NusA with TyIKR1 and RifDH10	S9
3. <b>Figure S9.</b> Chiral GC-MS analysis of the incubation of (2 <i>RS</i> )-2-methyl-3-ketopentanoyl-RifACP10-NusA with EryKR6 and RifDH10	S10
4. <b>Figure S10.</b> Chiral GC-MS analysis of the incubation of (2 <i>RS</i> )-2-methyl-3-ketopentanoyl-RifACP10-NusA with EryKR1 and RifDH10	S11
<b>Figure S11.</b> LC-ESI(+)-MS analysis of ( <i>E</i> )-2-methyl-2-pentenoyl-RifACP10	S12
<b>Incubations with EryACP6-bound substrates</b>	
1. <b>Figure S12.</b> TLC-phosphorimaging of diketide acid products	S13
2. <b>Figure S13.</b> GC-MS analysis of the incubation of <i>in situ</i> -generated (2 <i>R</i> )-2-methyl-3-ketopentanoyl-EryACP6 with TyIKR1, NADPH, and RifDH10	S14
3. <b>Figure S14.</b> Chiral GC-MS analysis of the incubation of <i>in situ</i> -generated (2 <i>R</i> )-2-methyl-3-ketopentanoyl-EryACP6 with RifDH10-KR10	S15
4. <b>Figure S15.</b> Chiral GC-MS analysis of the incubation of <i>in situ</i> -generated (2 <i>R</i> 4 <i>S</i> 5 <i>R</i> )-2,4-dimethyl-3-keto-5-hydroxyheptanoyl-EryACP6 with TyIKR1 and RifDH10	S16
5. <b>Figure S16.</b> Chiral GC-MS analysis of the incubation of ( <i>E</i> )-2-methylpentenoyl-EryACP6 with RifDH10	S17
<b>Incubations with acyl-S-NAC and acyl-S-pantetheine thioesters</b>	
1. <b>Synthesis of acyl-S-NAC and acyl-S-pantetheine thioesters</b>	S18
2. <b>Figure S17.</b> RifDH10-catalyzed dehydration/hydration of acyl thioester analogues	S20
3. <b>Incubation of <i>trans</i>-2-methyl-2-butenoyl-S-pantetheine (11) with RifDH10</b>	S20

4. <b>Figure S18.</b> Dehydration of (3 <i>R</i> )-3-hydroxybutanoyl-S-NAC	S21
5. <b>Figure S19.</b> Dehydration of (2 <i>R</i> ,3 <i>R</i> )-2-methyl-3-hydroxypentanoyl-S-NAC	S22
6. <b>Figure S20.</b> Dehydration of (2 <i>R</i> ,3 <i>R</i> )-2-methyl-3-hydroxypentanoyl-S-pantetheine	S23
7. <b>Figure S21.</b> Hydration of ( <i>E</i> )-2-butenoyl-S-pantetheine	S24
8. <b>Figure S22.</b> Hydration of ( <i>E</i> )-2-methyl-2-butenoyl-S-pantetheine	S25
9. <b>Figure S23.</b> Hydration of ( <i>E,E</i> )-2,4-hexadienoyl-S-pantetheine	S26
10. <b>Figure S24.</b> Stereochemistry of hydrated product from RifDH10-catalyzed hydration of ( <i>E</i> )-2-methyl-2-butenoyl-S-pantetheine	S27
11. <b>Method for thioester exchange of (2<i>R</i>,3<i>R</i>)-2-methyl-3-hydroxy-butanoyl-S-pantetheine to S-NAC</b>	S27
<b>Supplemental References</b>	S28

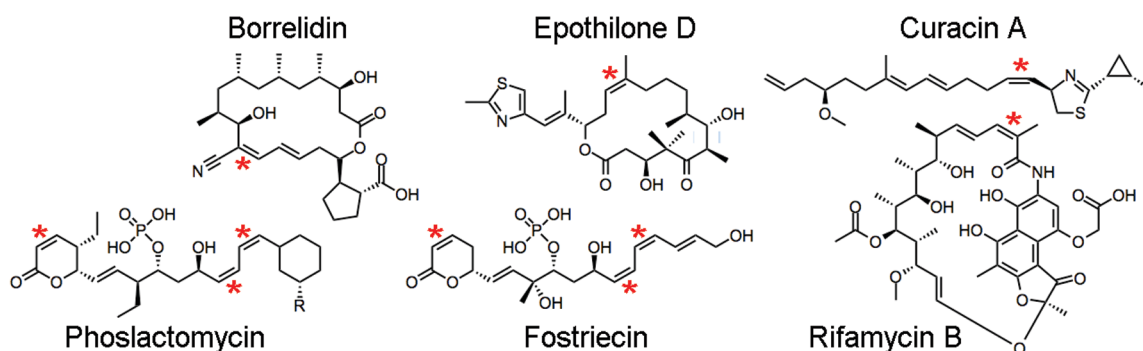


**Figure S1.** Polyketides with *cis* double bonds

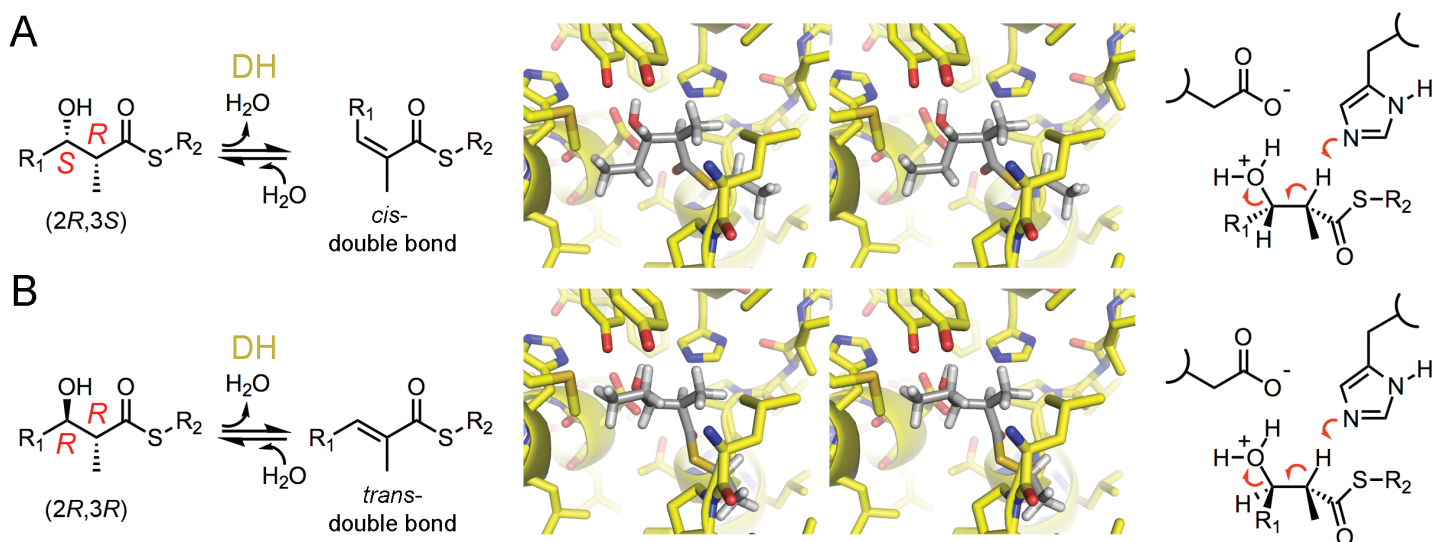


**Figure S2.** Dehydration of (2*R*,3*S*)- and (2*R*,3*R*)-2-methyl-3-hydroxyacyl thioesters. A) The *syn* dehydration of a (2*R*,3*S*) intermediate would result in a *cis*-enoyl thioester. The stereodiagram shows how the C2 proton and the C3 hydroxyl group of a (2*R*,3*S*)-2-methyl-3-hydroxypentanoyl intermediate would be aligned within the active site of RifDH10 for the *syn* elimination reaction. B) The *syn* dehydration of a (2*R*,3*R*) intermediate would result in a *trans*-enoyl thioester. The stereodiagram shows how the C2 proton and the C3 hydroxyl group of a (2*R*,3*R*)-2-methyl-3-hydroxypentanoyl intermediate would be aligned in the active site of RifDH10 for the *syn* elimination reaction.

## Domain boundaries and design of recombinant RifDH10 and RifACP10

```

1      MATDEKLLKYLKRVTAELHSLRKQGARHADEPLAVVGMACRFPPGGVSSPEDLWQLVAGGV
(.....Rifamycin PKS module 9.....)
1621   VLGHAGPEAVRADTAFKDTGFDSLTSVELRNRLREASGLKLPATLVFDYPTPVALARYLR
1681   DELGDTVATTPVATAAAAADAGEPIAIVGMACRLPGGVTDPEGLWRLVRDGLEGLSPFPED
1741   RGWDLLENLFDDDPDRSGTTYTSRGGFLDGAGLFDAGFFGISPREALAMPQQRLLLEAAW
1801   EALEGTGVDPGSLKGADVGVFAGVSNQGYGMGADPAELAGYASTAGASSVVSGRVSYVFG
1861   FEGPAVTIDTACSSSLVAMHLAGQALRQGECSMALAGGVTVMGTPGTFVEFAKQRLAGD      RifKS10
1921   GRCKAYAEGADGTGWAEGVGVVLERLSVARERGHRVLAVLRGSAVNSDGASNGLTAPNG
1981   PSQQRVIRRALAGAGLEPSDVIDIVEGHGTGTALGDPIEAQALLATYKDRDPETPLWLGS
2041   VKSNFGHTQSAAGVAGVIKMQALRHGVMPPTLHVDRPTSQVDWSAGAVEVLTEAREWPR
2101   NGRPRRAGVSSFGISGTNAHLIIIEEAPAEPQLAGPPPDDGGVVPLVVSARSPGALAGQARR
2161   LATFLGDGPLSDVAGALTSRALFGERAVVADSAAEEARAGLGALARGEDAPGLVRGRVPA
2221   SGLPGKLVWVFPQGTQWVGMGRELLEESPVFAERIAECAAALEPWIGWSLFDVLRGDGD
2281   LDRVDVLQPACFAVMVGLAAVWSSAGVVPDAVLGHSQGEIAAACVSGALSLEDAAKVVAL
2341   RSQAIAAKLSGRGGMASVALGEADVSRDLADGVEVAAVNGPASVVIAGDAQALDETLEAL      RifAT10
2401   SGAGIRARRVAVDYASHTRHVEDIEDTLAEALAGIDARAPLVFPLSTLTGEWIRDEGVVD
2461   GGYWYRNLRGRVRFGPAVEALLAQGHGVFVELSAHPVLVQPI TELTDETA AVVTGSLRRD
2521   DGGLRRLLTSMAE LFVRGVEVDWTSLVPPARADLPTYAFDHEHYWLRADTASDAVSLGL
2581   AGADHPLLGA VVQLPQSDGLVFTSRLSLRSHPLADHAVRDVVI VPGTGLVELAVRAGDE
2641   AGCPVLDLVEI EAPLVVPRGGVRVQVALGGPADDGSR TVDVFSLREDADSWLRHATGVL      RifDH10
2701   VPENRPRGTAAFDFAAWPPPEAKPVDLTGAYDVLADVG YGYGPTFRAVRAVWRRGSGNTT
2761   ETFAEIALPEDARAEAGRFGIHPALLDAALHSTMVSAADTESY GDEVRLPFAWNGLR LH
2821   AAGASVLRVRVAKPERDLSLEAVDESGGLVVTLD SLVGRPVSNDQLTTAAGPAGAGSLY
2881   RVDWTP LSSVDTSGRVPSWLPVATAEEVATLADDVLTGATEAPAVAVMEAVADEGSVLAL
2941   TVRVL DVVQCWLAGGGLEGTKLAI VTRGAVPAGDGVVHDPAAA AVWGLVRAAQAENPDR I
3001   VLLDVEPEADV PPLGSLVADGEPQVAVRGTTLSI PRLARAARPDPAAGFKTRGPVLVTG
3061   GTGSLGGLVARHLVERHGVRQLVLASRRGLDAEGAKDLVTDLTALGADVAVAACDVADRD      RifKR10
3121   QVAALLTEHRPSAVVHTAGVPDAGVIGTVTPDRLAEVFAPKVTAARHLDELTRDLDLDSF
3181   VVYSSVSAVFMGAGSGSYAAANAYLDGLMAHRRRAAGLPGQSLAWGLWDQTTGGMAAGTDE
3241   AGRARMTRRGGLVAMKPAAGLDFDAAIGSGEPLL VPAQLDLRGLRAEAAGGTEVPHLLR
3301   GLVRAGRQQARAAS TVEENWAGRLAGLEPAERGQV LLELVRAQVAGVLYRAAHQVDPDQ      RifACP10
3361   GLFEIGFDSLTAIELRNRLRARTERKISPGVVFDHPTPALLAAHLNELLRKKV 3413

```

**Figure S3.** Rifamycin PKS partial module 9 and module 10. Rifamycin polyketide synthase [*Amycolatopsis mediterranei* U32] Sequence ID: [ref|YP\\_003762843.1|](#) Length: 3413

ADTASDAVSLGLAGADHPLLGAVVQLPQSDGLVFTSRLSLRSHPLADHAVRDVVI VPGT  
GLVELAVRAGDEAGCPVLDELVIEAPLVVPRGGVVRVQVALGGPADDGSRTVDVFSLRED  
ADSWLRHATGVLVPENRPRGTAAAFDFAAWPPPEAKPVDLTGAYDVLADVGYGYGPTFRAV  
RAVWRRGSGNTTTETFAEIALPEDARAEAGRFGIHPALLDAALHSTMVSAAADTESYGDEV  
RLPFAWNGRLRLHAAGASVLRVVRVAKPERDLSLSLEAVDESGGLVVTLDSLVRPVSNDQLT  
TAAG

ATGGCGGACACGGCAAGCGACGCAGTAAGCCTCGGCCTGGCAGGTGCGGATCACCCGCTGCTGGGTGCAGTCGTGCAATTG  
CCGCAGAGCGATGGCCTGGTCTTTACGTCCCCTTGAGCCTGCGCTCCCATCCGTGGTTGGCGGATCACGCGGTTCCGCGAC  
GTTGTTATTGTGCCGGGCACTGGTCTGGTTGAACTGGCCGTCCGTGCTGGCGACGAAGCCGGCTGCCCGGTGCTGGATGAG  
CTGGTGATCGAAGCGCCGCTGGTCTGCCGCTCGTGGCGGTGTGCGTGTTC AAGTCGCACTGGGTGGTCCGGCGGATGAC  
GGTTCGCGCACCGTTGACGTCTTTAGCCTGCGTGAGGACGCCGATAGCTGGCTGCGTCACGCTACCGGTGTGCTGGTTCCA  
GAGAATCGTCCGCGTGGTACCGCTGCCTTCGATTTTGC GCGGTGGCCTCCGCCGGAAGCGAAGCCGGTCGACCTGACGGGC  
GCATACGATGTTTTGGCGGACGTTGGTTACGGTTATGGCCCGACGTTCCGCGCAGTGCGTGCCGTGTGGCGTCGCGGCTCC  
GGTAACACCACCGAAACCTTTGCGGAGATCGCGCTGCCGGAGGACGCGCGTGCGGAGGCAGGCCGTTTCGGTATTCATCCG  
GCACTGCTGGATGCCGCGCTGCATAGCACCATGGTCAGCGCCGCTGCGGATAACCGAGAGCTATGGCGATGAAGTTCGTCTG  
CCGTTCGCATGGAATGGTTTGC GCGCTGCACGCGGCTGGTGCAGCGTCCTGCGTGTGCGCGTTGCCAAACCAGAACGCGAT  
AGCCTGAGCCTGGAGGCGGTTGACGAGTCTGGTGGCTTGGTTGTGACGCTGGACTCTCTGGTGGGTGCTCCTGTGAGCAAC  
GACCAGCTGACCACTGCAGCGGGT

N-terminus: CATATG (NdeI site)  
C-terminus: TAACTCGAG (Stop codon/XhoI)

**Figure S4.** RifDH10 amino acid sequence. The synthetic gene encoding RifDH10 domain was subcloned in the pET-28a vector and the recombinant protein was expressed with a N-terminal His<sub>6</sub>-tag in *E.coli* BL21 (DE3). Protein expression and purification procedures are described below.

LAGLEPAERGOVLLELVRAQVAGVLGYRAAHQVDPDQGLFEIGFDSLTAIELRNRLRART  
ERKISPGVVFDPHPTALLAAHLNELL

ATGCTGGCCGGCCTGGAACCTGCAGAACGCGGTCAAGTCCTGCTGGAGCTGGTGCCTGCGCAGGTTGCGGGCGTGCTGGGC  
TACCGTGCTGCCCATCAGGTTGACCCGGATCAAGGTCTGTTTCGAGATCGGTTTTGACAGCCTGACGGCGATCGAGCTGCGC  
AACCGTTTTGCGTGCGCGCACCGAAGTAAGATTAGCCCGGGTGTGTTTTTCGATCACCCGACTCCGGCGTTGCTGGCAGCA  
CACTTGAATGAGCTGCTG

N-terminus: CATATG (NdeI site)

**Figure S5.** RifACP10 amino acid sequence. The synthetic gene encoding RifACP10 was initially ligated into the NdeI/XhoI sites of pET-28a. Since the resultant recombinant RifACP10 was obtained only as insoluble inclusion bodies when expressed in *E.coli* BL21 (DE3), the corresponding RifACP10-NusA protein was constructed.

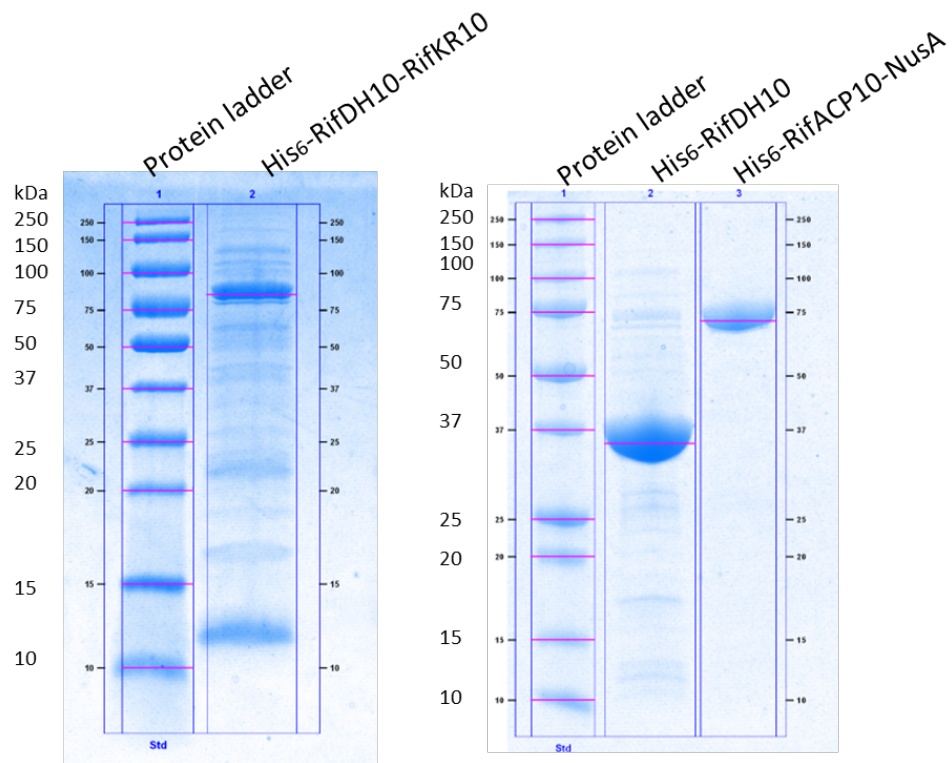


**Figure S6.** SDS-PAGE of recombinant RifDH10-KR10, RifDH10 and RifACP10-NusA

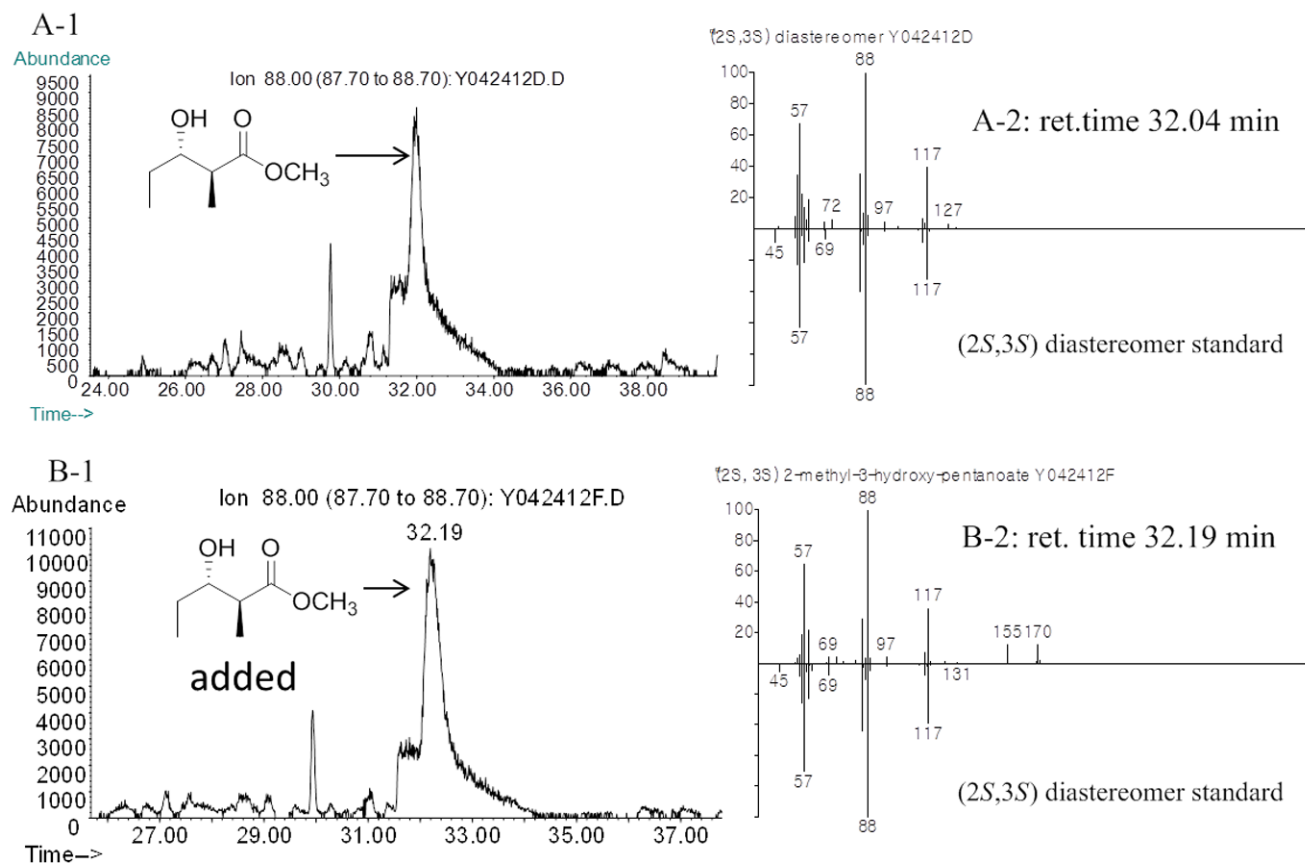


**Figure S7.** Chiral GC-MS analysis of the incubation of (2RS)-2-methyl-3-ketopentanoyl-RifACP10-NusA with RifKR7 in the absence of RifDH10 (Method 4). **A:** Methyl (2S,3S)-2-methyl-3-hydroxypentanoate (**4a**) from RifKR7-catalyzed reduction of (2RS)-2-methyl-3-ketopentanoyl-RifACP10-NusA and **B:** Co-injection of (2S,3S)-**4a** with A. **A-1 and B-1:** Extracted ion current (XIC) at  $m/z$  88 (base peak). **A-2 and B-2:** Mass spectra of selected peak corresponding to (2S,3S)-**4a** upper half, observed spectra, lower half, inverted mass spectra of reference standard.



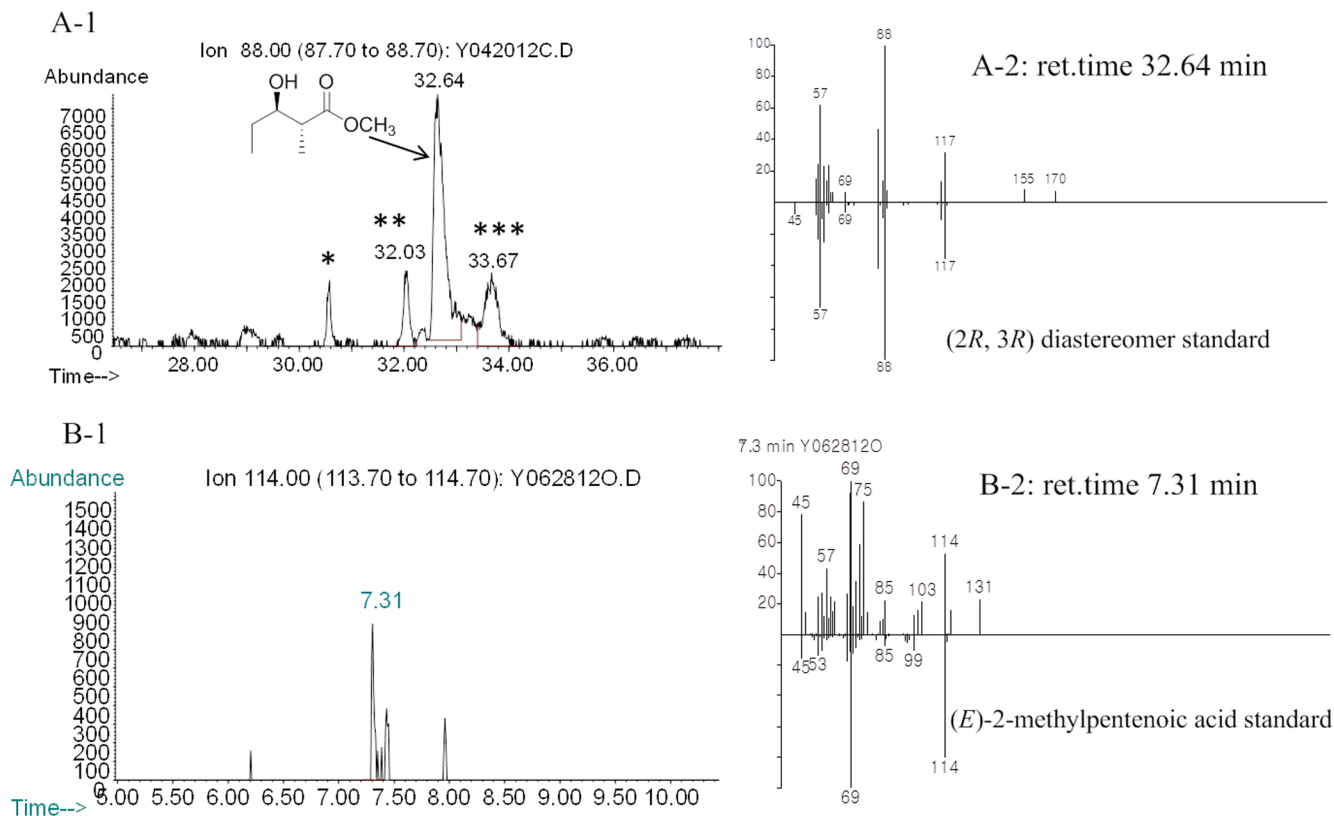


**Figure S8.** Chiral GC-MS analysis of the incubation of (2RS)-2-methyl-3-ketopentanoyl-RifACP10-NusA with TyIKR1 and RifDH10 (Methods 2 and 4). **A:** Methyl 2-methyl-3-hydroxy-pentanoates from TyIKR1-catalyzed reduction of (2RS)-2-methyl-3-ketopentanoyl-RifACP10-NusA and **B:** Minor peak corresponding to (E)-2-methyl-2-pentenoic acid (**3**) generated by RifDH10-coupled dehydration of A. **A-1:** Extracted ion current (XIC) at  $m/z$  88 (base peak). The major diastereomer observed was (2R,3R)-**4b**. The minor diastereomers are marked with asterisks as (2R,3S)-**4c** (\*), (2S,3R)-**4d** (\*\*) and (2S,3S)-**4a** (\*\*\*). **A-2:** mass spectra of selected peak corresponding to (2R,3R)-**4b**, upper half, observed spectrum, lower half, inverted mass spectrum of reference standard. **B-1:** Extracted ion current (XIC) at  $m/z$  114 (base peak). **B-2:** Mass spectrum of selected peak, upper half, observed spectrum, lower half, inverted mass spectra of reference standard. (Note both the lower intensity and lower purity of the ret. time 7.31 min peak containing **3** plus contaminants, compared to the yield and purity of **3** derived from an incubation carried out in the presence of RifKR7 (cf Figure 3))

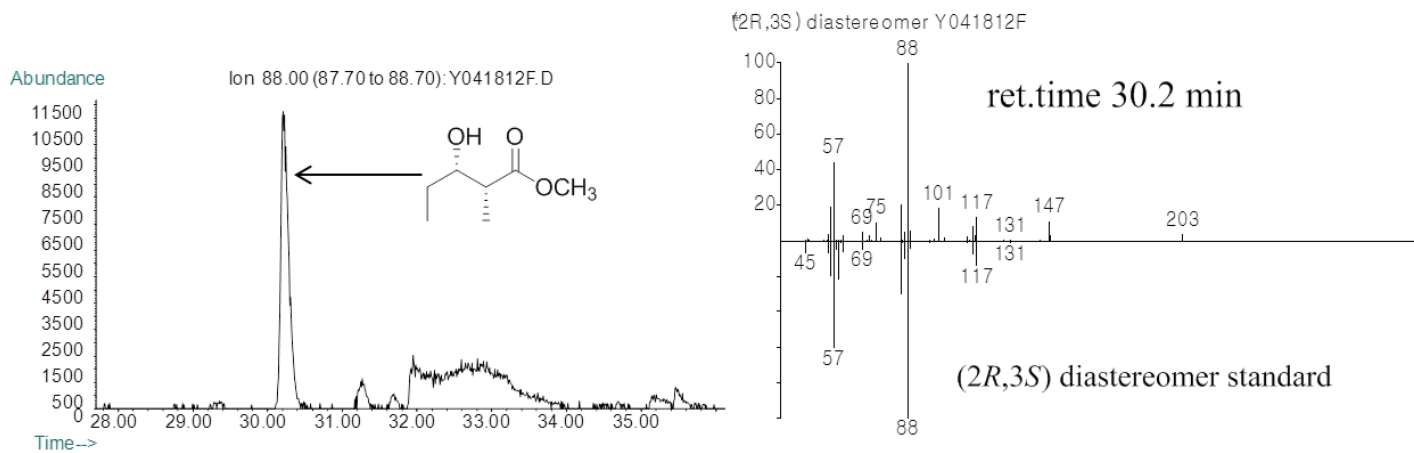


**Figure S9.** Chiral GC-MS analysis of the incubation of (2*RS*)-2-methyl-3-ketopentanoyl-RifACP10-NusA with EryKR6 and RifDH10 (Method 4). **Left panel:** Extracted ion current (XIC) at  $m/z$  88 (base peak). **Right panel,** mass spectra of a selected peak corresponding to (2*R*,3*S*)-**4c**, upper half, observed spectrum, lower half, inverted mass spectrum of reference standard. No dehydration product **3** was observed.

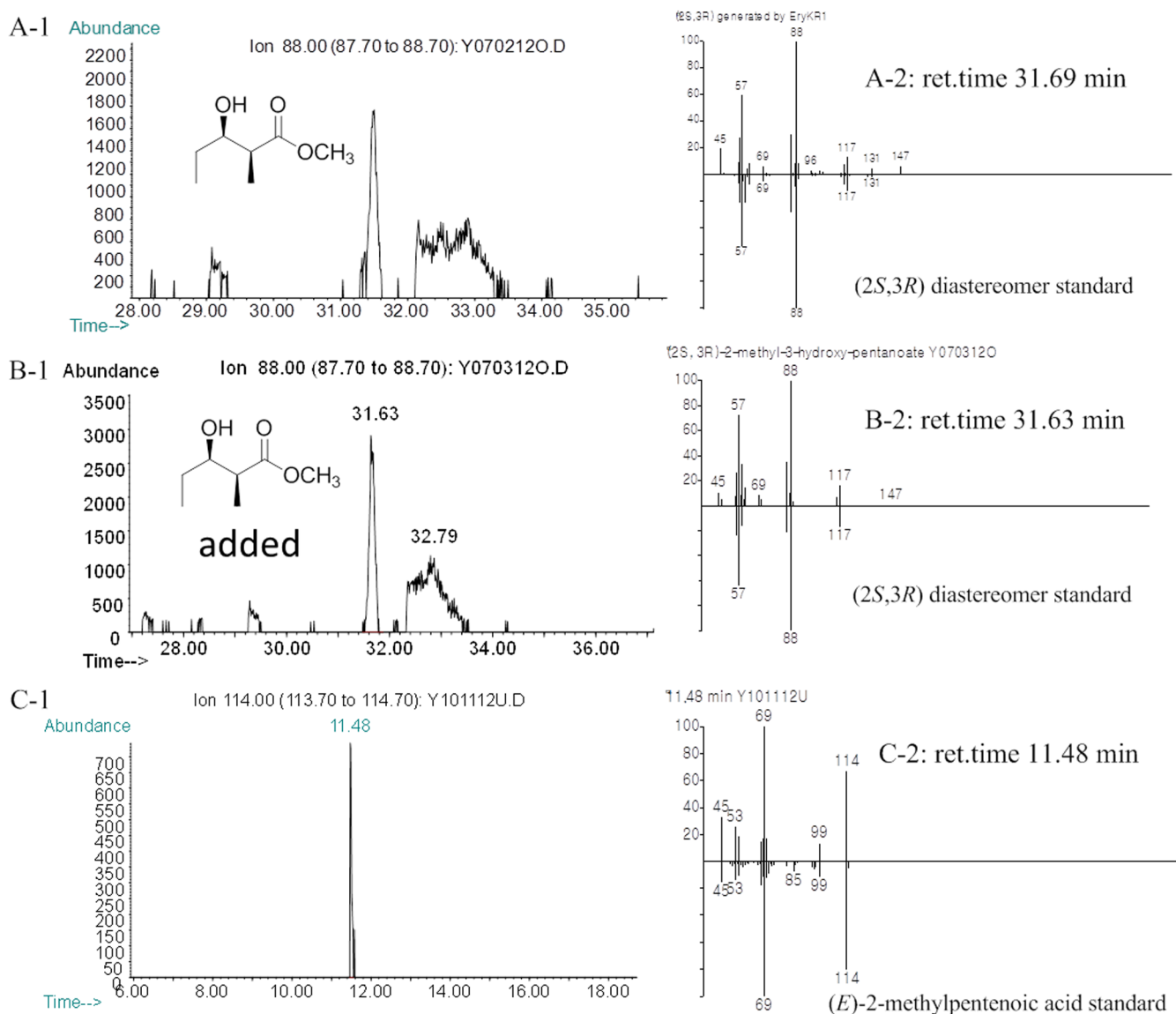


**Figure S10.** Chiral GC-MS analysis of the incubation of (2RS)-2-methyl-3-ketopentanoyl-RifACP10-NusA with EryKR1 and RifDH10. **A:** Methyl 2-methyl-3-hydroxypentanoates from EryKR1-catalyzed reduction of (2RS)-2-methyl-3-ketopentanoyl-RifACP10-NusA (Method 4) and **B:** Co-injection of (2S,3R)-**4d** diastereomer with A. Envelope at 32.79 min contains minor amounts of (2S,3S)-**4a**. **C:** Minor amount of **3** generated by RifDH10-coupled reaction of A, due to presence of (2S,3S)-**1a** in reduced RifACP10-bound diketide. (Method 1) **A-1** and **B-1:** Extracted ion current (XIC) at  $m/z$  88 (base peak). **A-2** and **B-2:** mass spectra of selected peak corresponding to (2S,3R)-**4d**, upper half, observed spectrum, lower half, inverted mass spectrum of reference standard. **C-1:** Extracted ion current (XIC) at  $m/z$  114 (base peak). **C-2:** mass spectrum of selected peak, upper half, observed spectrum, lower half, inverted mass spectrum of reference standard **3**.

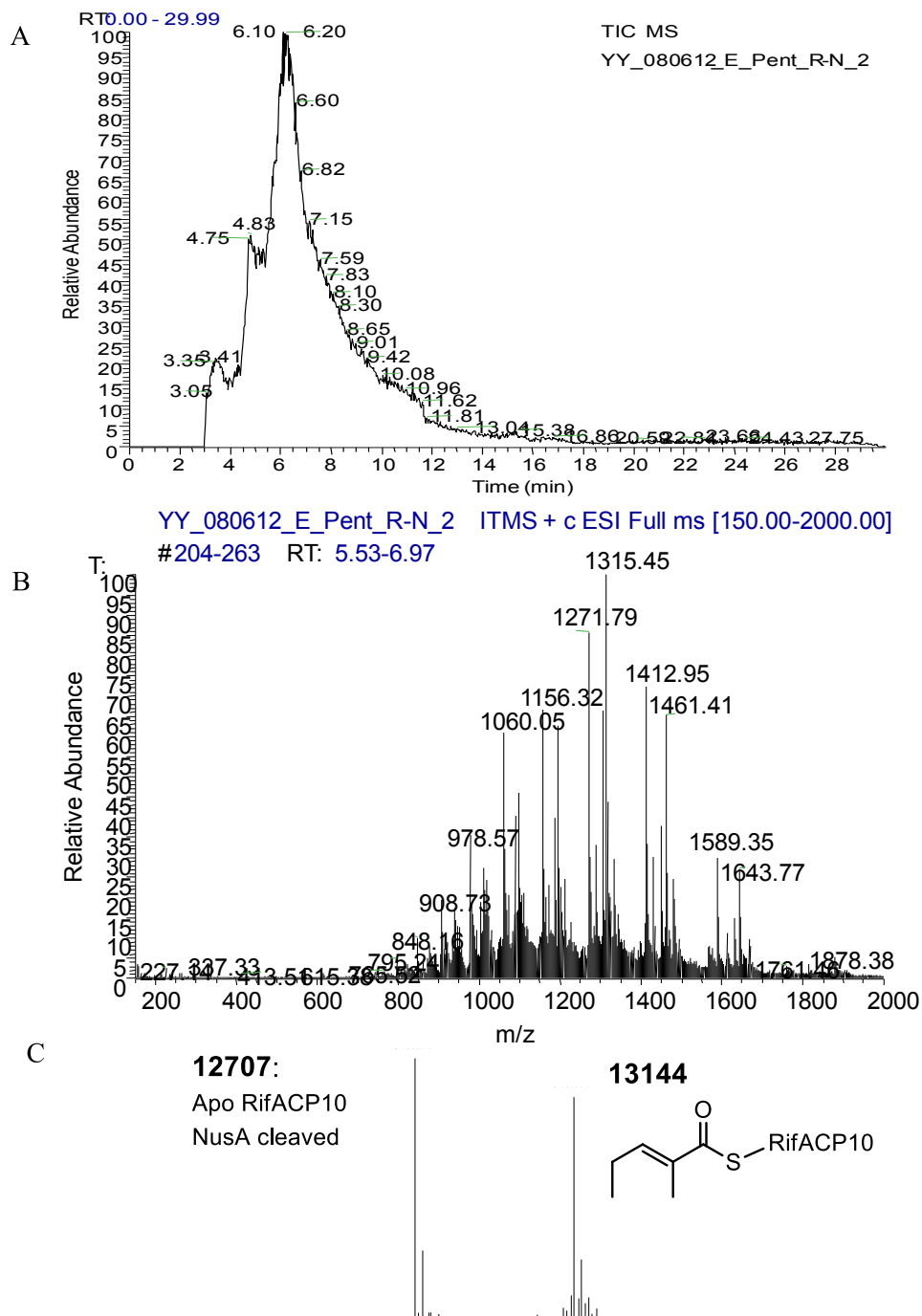
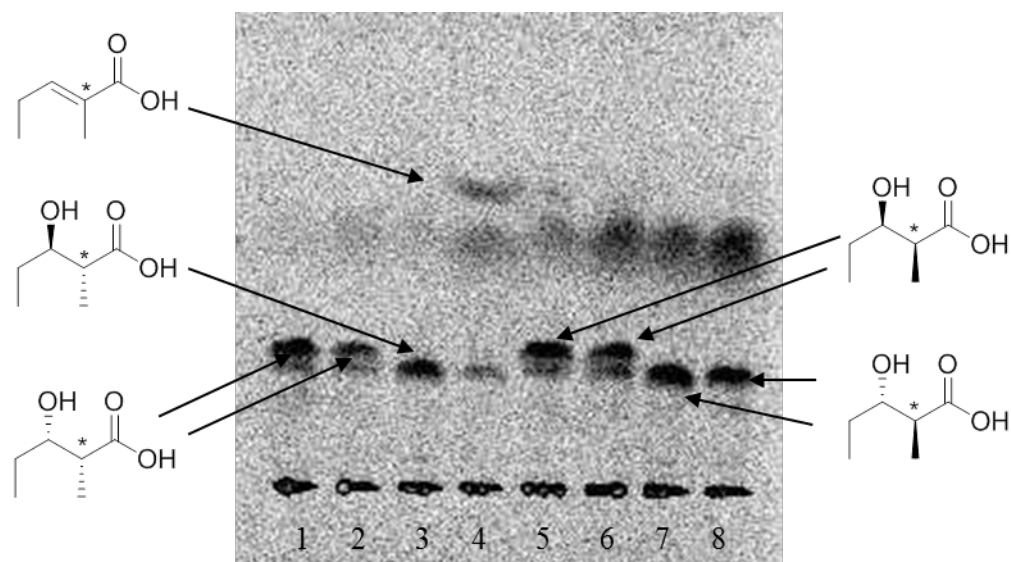


**Figure S11.** LC-ESI(+)-MS analysis of (*E*)-2-methyl-2-pentenoyl-RifACP10 generated by incubation of (*E*)-2-methylpentenoyl-CoA with Sfp and *apo*-RifACP10-NusA, followed by proteolytic cleavage of the NusA fragment with HRV 3C protease. **A.** LC-MS; **B.** LC-ESI(+)-MS; **C.** calculated full mass of (*E*)-2-methylpentenoyl-RifACP10 (theoretical  $[M+H]^+$  13143.9 Da). *apo*-RifACP10 was also observed (theoretical mass  $[M+H]^+$  12706.7 Da).



	EryKR6	TylKR1	EryKR1	RifKR7	RifDH10
1	+	-	-	-	-
2	+	-	-	-	+
3	-	+	-	-	-
4	-	+	-	-	+
5	-	-	+	-	-
6	-	-	+	-	+
7	-	-	-	+	-
8	-	-	-	+	+

**Figure S12.** TLC-phosphorimaging of diketide acid products from combinatorial enzyme reactions involving propionyl-SNAC, Ery[KS6][AT6], EryACP6, RifDH10, [<sup>14</sup>C]-methylmalonyl-CoA, NADPH, and varying KR domains. Only Expt 4 with TylKR1 and RifDH10 produced 2-methyl-2-pentenoic acid. Note that the achiral TLC assay cannot distinguish *syn*-(2*S*,3*R*)- from the enantiomeric *syn*-(2*R*,3*S*)-2-methyl-3-hydroxypentanoic acid nor *anti*-(2*S*,3*S*)- from the enantiomeric *anti*-(2*R*,3*R*)-2-methyl-3-hydroxypentanoic acid.

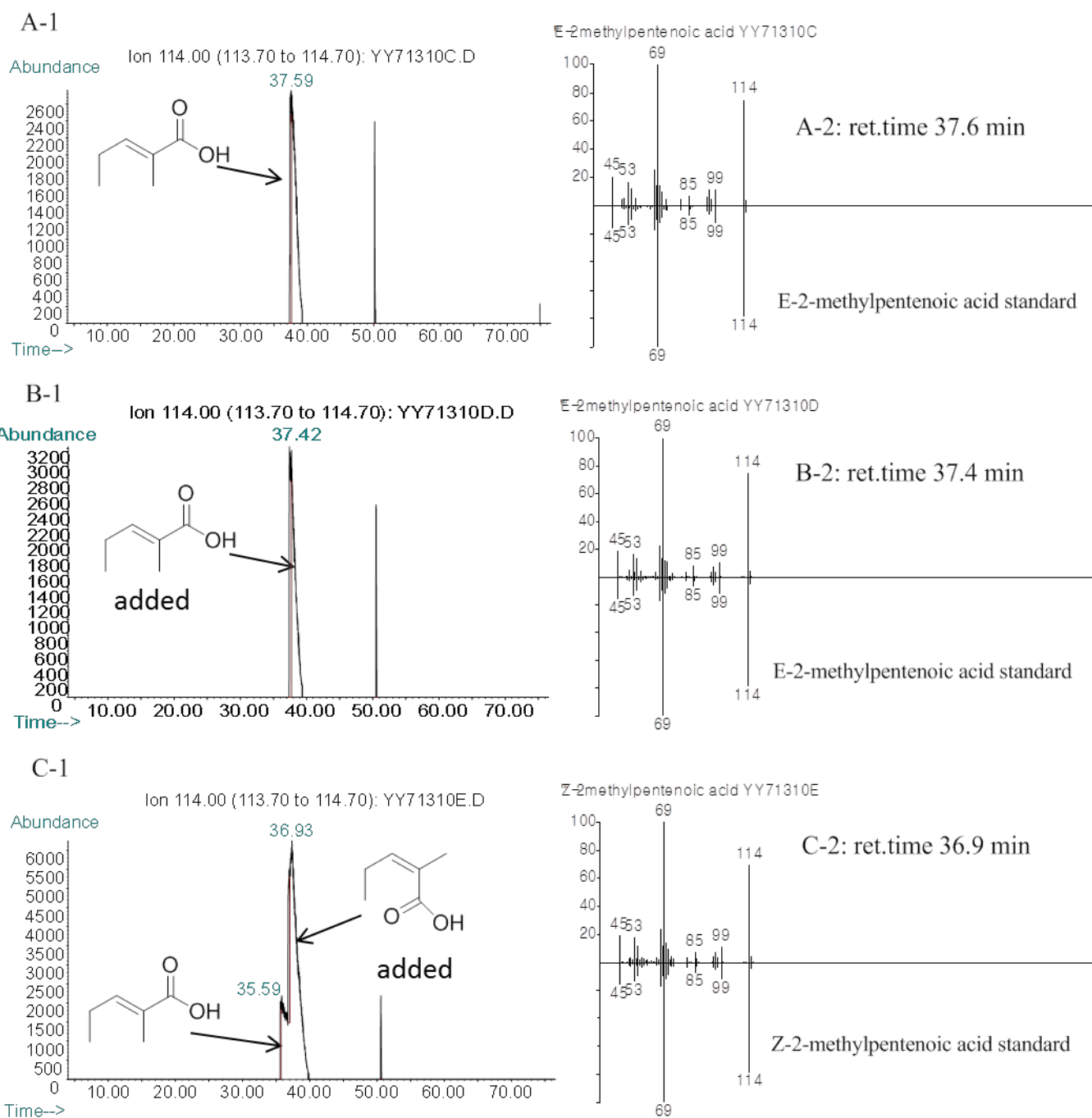
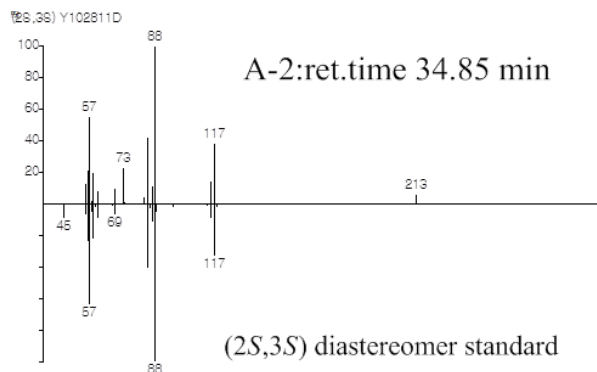
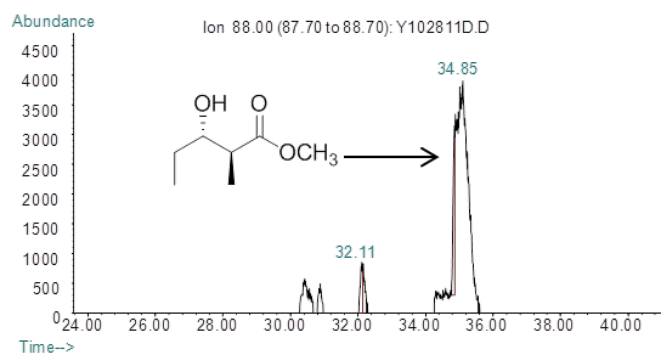


**Figure S13.** GC-MS analysis of the incubation of *in situ*-generated (2*R*)-2-methyl-3-ketopentanoyl-EryACP6 with TylKR1, NADPH, and RifDH10 (Method 3). **Left panels:** Extracted ion current (XIC) at *m/z* 114 (base peak). **Right panels,** mass spectra of selected peaks corresponding to unsaturated diketide acid **3**, upper half, observed peaks, lower half, mass spectrum of reference standard **3**. **A.** Reaction product. **B.** A plus authentic (*E*)-**3**. **C.** A plus authentic (*Z*)-2-methyl-2-pentenoic acid.

A-1



B-1

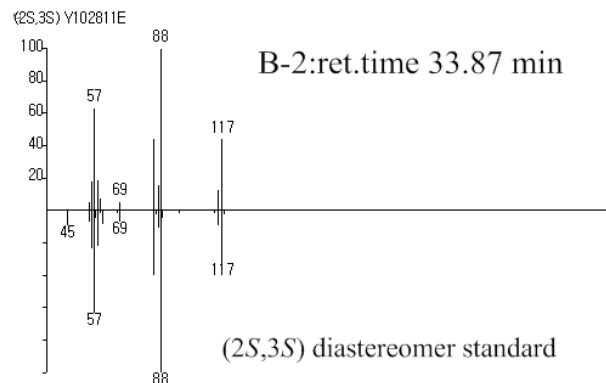
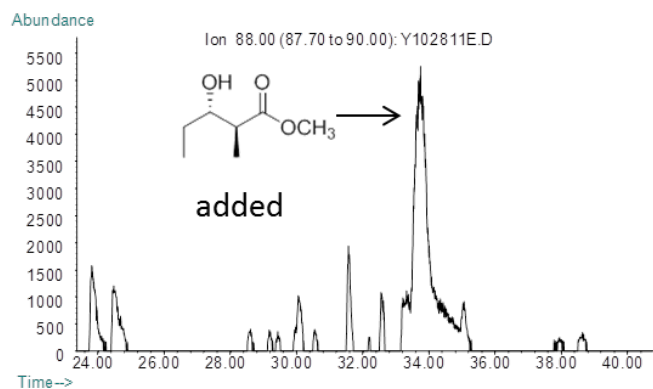


**Figure S14.** Chiral GC-MS analysis of the incubation of *in situ*-generated (2*R*)-2-methyl-3-ketopentanoyl-EryACP6 with RifDH10-KR10 (Method 4). Formation of methyl (2*S*,3*S*)-2-methyl-3-hydroxypentanoate. **Left panels:** Extracted ion current (XIC) at *m/z* 88 (base peak). **Right panels,** mass spectra of selected peaks corresponding to **4a**, upper half, observed spectrum, lower half, inverted mass spectrum of reference standards. **A** (2*S*,3*S*)-**4a** generated by RifDH10-KR10. **B.** A plus (2*S*,3*S*)-**4a** generated by enzymatic incubation by RifKR7 alone. No dehydration products such as **3** could be detected.

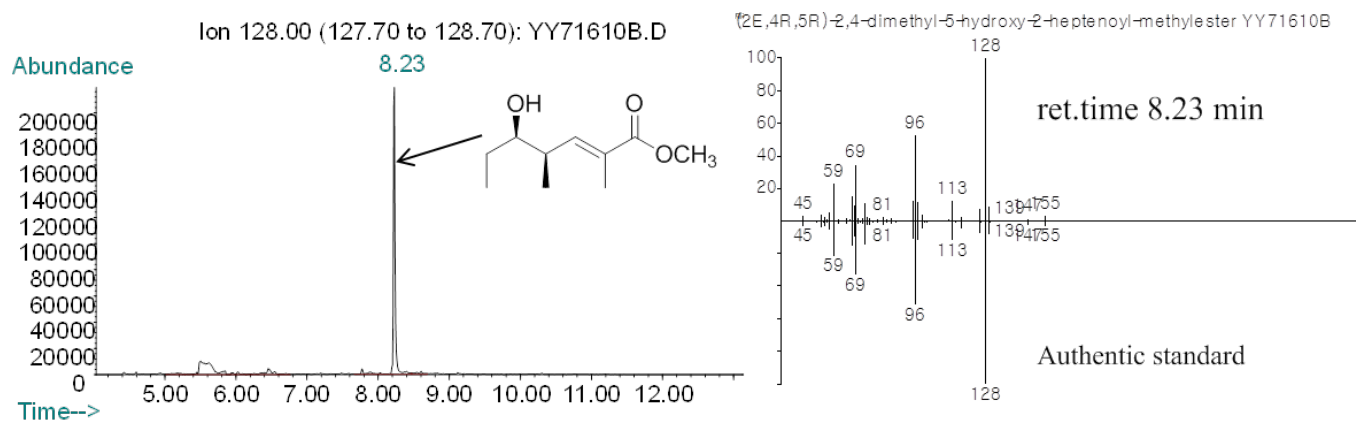


**Figure S15.** Chiral GC-MS analysis of the incubation of *in situ*-generated (2*R* 4*S* 5*R*)-2,4-dimethyl-3-keto-5-hydroxyheptanoyl-EryACP6 with TyIKR1 and RifDH10. Reaction produces (2*E*,4*R*,5*R*)-2,4-dimethyl-5-hydroxy-2-heptenoyl methyl ester resulting from dehydration of the intermediate (2*R*,3*R*,4*S*,5*R*)-2,4-dimethyl-3,5-dihydroxyheptanoyl-EryACP6, hydrolysis, and methylation. **Left panel:** Extracted ion current (XIC) at *m/z* 128 (base peak for (2*E*,4*R*,5*R*)-2,4-dimethyl-5-hydroxy-2-heptenoyl methyl ester). **Right panel:** mass spectrum of selected peak corresponding to the unsaturated triketide acid methyl ester, upper half, observed peak, lower half, mass spectrum of reference standard.



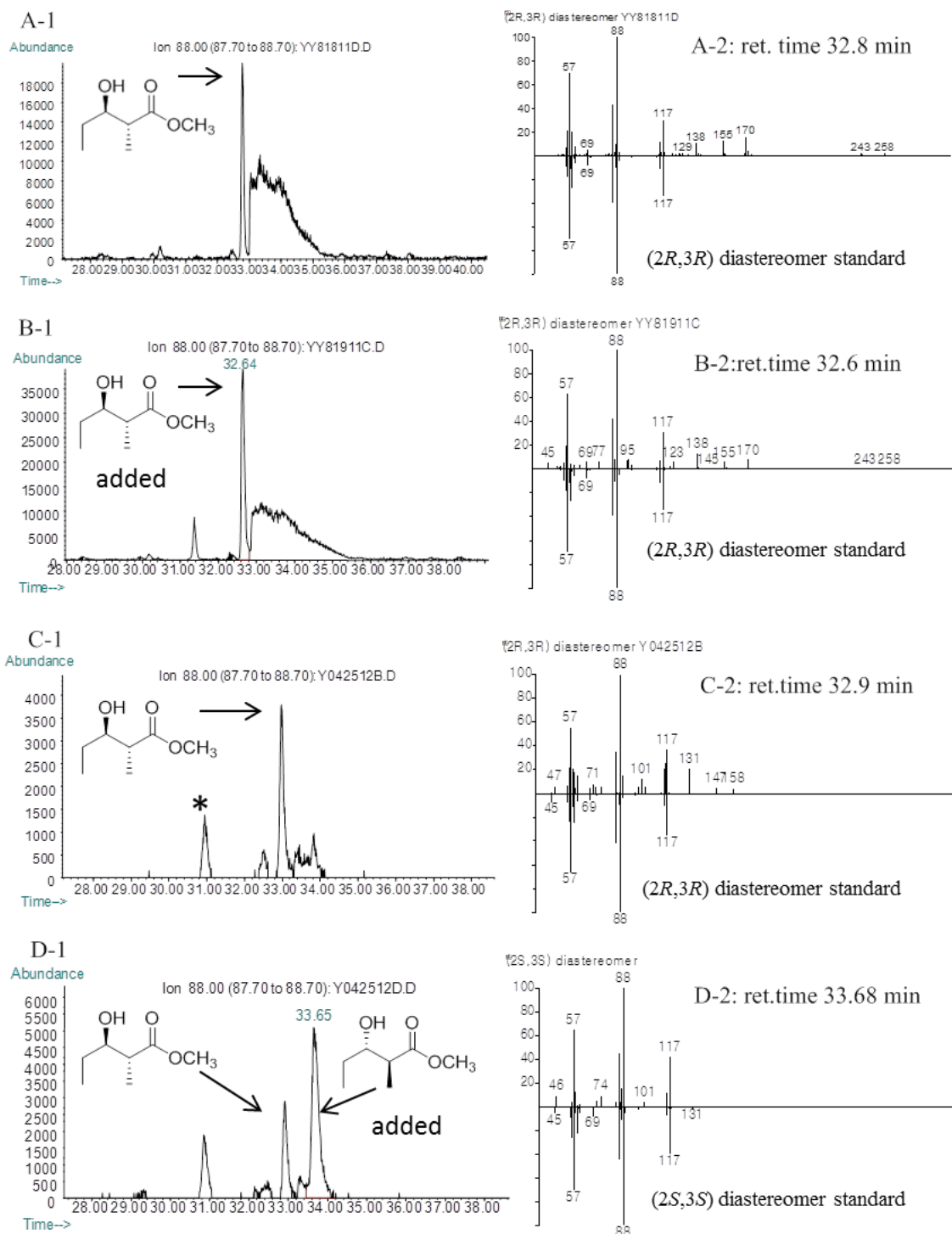


**Figure S16.** Chiral GC-MS analysis of the incubation of (*E*)-2-methylpentenoyl-EryACP6 with RifDH10 (Method 4). **Left panels:** Extracted ion current (XIC) at *m/z* 88 (base peak). **Right panels,** mass spectra of selected peaks corresponding to diastereomers, upper half, observed spectrum, lower half, inverted mass spectrum of reference standard. **A** and **C.** (*2R,3R*)-**4b** produced by RifDH10. **B.** A plus (*2R,3R*)-**4b** standard. **D.** C plus (*2S,3S*)-**4a** standard.

## Synthesis of acyl-S-NAC and acyl-S-pantetheine thioesters

**NMR and LC-MS characterization of S-pantetheine esters.**  $^1\text{H}$  NMR analysis of S-pantetheine esters was performed on a Varian Mercury 400 MHz instrument. LC-MS was performed on an Agilent Technologies 1200 Series HPLC with a Gemini  $\text{C}_{18}$  column (5  $\mu\text{m}$ , 2  $\times$  50 mm; Phenomenex) coupled to an Agilent Technologies 6130 quadrupole mass spectrometer system equipped with an electrospray-ionization source. A 5–95% B gradient over 12 min at a flow rate of 0.7 mL/min was run in which the mobile phases were (A)  $\text{H}_2\text{O}$  with 0.1% formic acid and (B) acetonitrile with 0.1% formic acid.

*N*-Acetylcysteamine (NAC), Meldrum's acid derivatives, the methylketene dimer, (2*RS*)-2-methyl-3-ketobutanoyl-S-NAC, (2*RS*)-2-methyl-3-ketopentanoyl-S-NAC, and (3*R*)-3-hydroxypentanoyl-S-NAC were synthesized as previously reported,<sup>1</sup> as was *trans*-2-butenoyl-S-pantetheine.<sup>2</sup>

**(2*RS*)-2-Methyl-3-ketopentanoyl-S-pantetheine.** Sodium borohydride (80 mg, 16 eq.) was added to 94 mg D-pantetheine (1 eq.) dissolved in 5 mL 80:20 MeOH:0.25 M  $\text{NaHCO}_3$  (aq.) over 20 min at 22 °C. After 1 h, the reaction was quenched by adding glacial acetic acid dropwise until bubbling ceased and then was buffered with 250 mM HEPES (pH 7.5). 11.2 mg (1.4 eq.) of methylketene dimer was added to the solution at 22 °C. After 1 h, the reaction was evaporated and salts were removed using a plug of silica gel (2% MeOH:dichloromethane). (2*RS*)-2-Methyl-3-ketopentanoyl-S-pantetheine:  $^1\text{H}$  NMR (400 MHz,  $\text{D}_2\text{O}$ )  $\delta$  0.71 (s, 3H), 0.74 (s, 3H), 0.81-0.88 (t, 3H,  $J = 8$  Hz), 1.20-1.25 (d, 3H,  $J = 8$  Hz), 2.28-2.33 (m, 2H) 2.51-2.58 (q, 2H,  $J = 8$  Hz), 2.90-2.97 (t, 2H,  $J = 7.2$  Hz), 3.20-3.26 (m, 2H), 3.30-3.40 (m, 2H), 3.40-3.45 (m, 2H), 3.81 (s, 1H), 4.00-4.05 (q, 1H,  $J = 8$  Hz). ESI-MS expected mass: 391.5, observed mass: 391.2.

**(2*R,3R*)-2-methyl-3-hydroxypentanoyl-S-pantetheine, (2*R,3S*)-2-methyl-3-hydroxypentanoyl-S-pantetheine, (2*S,3R*)-2-methyl-3-hydroxypentanoyl-S-pantetheine, and (2*S,3S*)-2-methyl-3-hydroxypentanoyl-S-pantetheine.** Each of the stereoisomers of 2-methyl-3-hydroxypentanoyl-S-pantetheine was prepared from the incubation of (2*RS*)-2-methyl-3-ketopentanoyl-S-pantetheine with various recombinant KR domains that have been shown to stereospecifically reduce the corresponding NAC-bound compounds (TylKR1, AmpKR2, EryKR1, and AmpKR1, respectively).<sup>1</sup> Reduction reactions were carried out in 10% (v/v) glycerol, 150 mM HEPES (pH 7.5), 100 mM NaCl, 200 mM D-glucose, 500  $\mu\text{M}$   $\text{NADP}^+$ , 10  $\mu\text{M}$  KR, 1  $\mu\text{M}$  GDH (cloned from *Bacillus subtilis*), and 2-10 mM (2*RS*)-2-methyl-3-ketopentanoyl-S-pantetheine in a total volume of 200  $\mu\text{L}$  for 24 h at 22 °C. The

reaction was monitored by TLC, and the reduction product was purified by silica gel chromatography with 1:1 ethyl acetate:acetone.

***trans*-2-Methyl-2-butenoyl-S-pantetheine (11).** D-pantetheine (1 mL of 0.5 M aq. soln) was reduced to D-pantetheine by addition of 75 mg DTT (1 eq.) and stirring for 1 h at 22 °C. Water was removed by vacuum to leave a clear, viscous liquid that was resuspended in 10 mL DCM. *trans*-2-Methyl-2-butenoyl-S-pantetheine (11): <sup>1</sup>H NMR (400 MHz, D<sub>2</sub>O) δ 0.71 (s, 3H), 0.74 (s, 3H), 1.66-1.70 (m, 6H), 2.29 (t, 3H, *J* = 6.5 Hz), 2.91 (t, 3H, *J* = 6.5 Hz), 3.20-3.36 (m, 8H), 3.81 (s, 1H), 6.80 (qq, 1H, *J*<sub>1</sub> = 1.0 Hz, *J*<sub>2</sub> = 6.6 Hz).

**3*R*-Hydroxybutanoyl-S-pantetheine.** RifDH10 (30 μM) was incubated with 10 mM *trans*-2-butenoyl-S-pantetheine in a 1 mL solution containing 150 mM NaCl, 10% (v/v) glycerol, 150 mM HEPES pH 7.5. After 24 h, the reaction was injected on a C<sub>18</sub> reversed-phase HPLC column (100% water with 0.1% TFA to 100% MeOH with 0.1% TFA, 30 min), and the peak corresponding to the hydrated species was collected and concentrated under vacuum. *3R-Hydroxybutanoyl-S-pantetheine*: <sup>1</sup>H NMR (400 MHz, D<sub>2</sub>O) δ 0.71 (s, 3H), 0.74 (s, 3H), 1.05 (d, 3H, *J* = 6.4 Hz), 2.29 (t, 3H, *J* = 6.5 Hz), 2.63 (d, 2H, *J* = 6.4 Hz), 2.89 (td, 2H, *J*<sub>1</sub> = 2.2 Hz, *J*<sub>2</sub> = 6.3 Hz), 3.21 (m, 3H), 3.32 (m, 3H), 3.46 (d, 1H, *J* = 4.4 Hz), 3.48 (d, 1H, *J* = 4.4 Hz), 3.81 (s, 1H), 4.09 (h, 1H, *J* = 6.5 Hz).

**(2*R*,3*R*)-2-Methyl-3-hydroxybutanoyl-S-pantetheine (12b).** Prepared in the same manner as *3R*-hydroxybutanoyl-S-pantetheine, substituting *trans*-2-methyl-2-butenoyl-S-pantetheine for *trans*-2-butenoyl-S-pantetheine. *(2R,3R)-2-Methyl-3-hydroxybutanoyl-S-pantetheine (12b)*: <sup>1</sup>H NMR (400 MHz, D<sub>2</sub>O) δ 0.71 (s, 3H), 0.74 (s, 3H), 0.96 (d, 3H, *J* = 7.1 Hz), 1.04 (d, 3H, *J* = 6.3 Hz), 2.29 (t, 3H, *J* = 6.5 Hz), 2.63 (dd, 3H, *J*<sub>1</sub> = 1.2 Hz, *J*<sub>2</sub> = 8.1 Hz), 3.20-3.36 (m, 8H), 3.81 (s, 1H).

***cis*-2-Methyl-2-butenoyl-S-pantetheine (13).** Prepared similarly to *trans*-2-butenoyl-S-pantetheine, substituting 100 mg of *cis*-2-methyl-2-butenoyl-S-pantetheine for *trans*-2-methyl-2-butenoyl-S-pantetheine. *cis*-2-Methyl-2-butenoyl-S-pantetheine (13): <sup>1</sup>H NMR (400 MHz, CDCl<sub>3</sub>) δ 0.95 (s, 3H), 1.06 (s, 3H), 1.28 (t, 3H, *J* = 7.1 Hz), 1.96 (dq, 3H, *J*<sub>1</sub> = 1.7 Hz, *J*<sub>2</sub> = 7.3 Hz), 2.02 (t, 3H, *J* = 2.0 Hz), 2.44 (t, 2H, *J* = 6.3 Hz), 3.11 (q, 2H, *J* = 6.7 Hz), 3.49-3.65 (m, 4H), 4.01 (d, 1H, *J* = 4.8 Hz), 4.14 (q, 3H, *J* = 7.4 Hz), 5.93 (qq, 1H, *J*<sub>1</sub> = 2.4 Hz, *J*<sub>2</sub> = 7.8 Hz).

***trans,trans-2,4-Hexadienoyl-S-pantetheine.*** *trans,trans-2,4-Hexadienoic acid* (1.0 g, Alfa Aesar) was stirred in 5 mL oxalyl chloride at 22 °C under a flow of nitrogen gas. After the oxalyl chloride had evaporated, reduced D-pantetheine (see synthesis of *trans-2-methyl-2-butenoyl-S-pantetheine* for D-pantetheine reduction protocol) dissolved in 8.5 mL DCM and 1.5 mL TEA was added to the activated acid, and set to stir at 0 °C for 1 h, followed by quenching with 2 mL methanol. The reaction was washed with brine and all solvent was removed under vacuum, leaving a viscous liquid that was purified by silica gel chromatography with 1:1 ethyl acetate:acetone. *trans,trans-2,4-Hexadienoyl-S-pantetheine*: <sup>1</sup>H NMR (400 MHz, D<sub>2</sub>O) δ 0.71 (s, 3H), 0.74 (s, 3H), 1.12 (t, 1H, *J* = 7.3 Hz), 1.71 (d, 2H, 6.6), 2.29 (t, 3H, *J* = 6.5 Hz), 2.96 (t, 3H, *J* = 6.5), 3.20-3.36 (m, 8H), 3.81 (s, 1H), 6.16 (m, 3H), 7.14 (dd, 1H, *J* = 10.6 Hz).

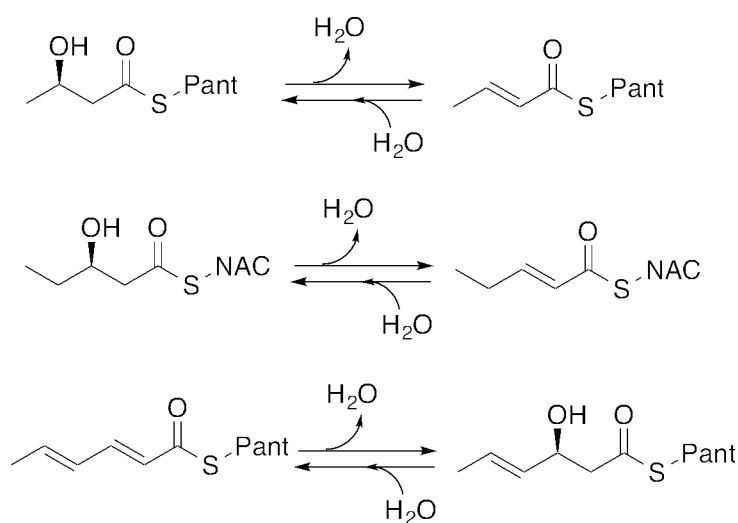


**Figure S17.** RifDH10-catalyzed dehydration/hydration of acyl thioester analogues.

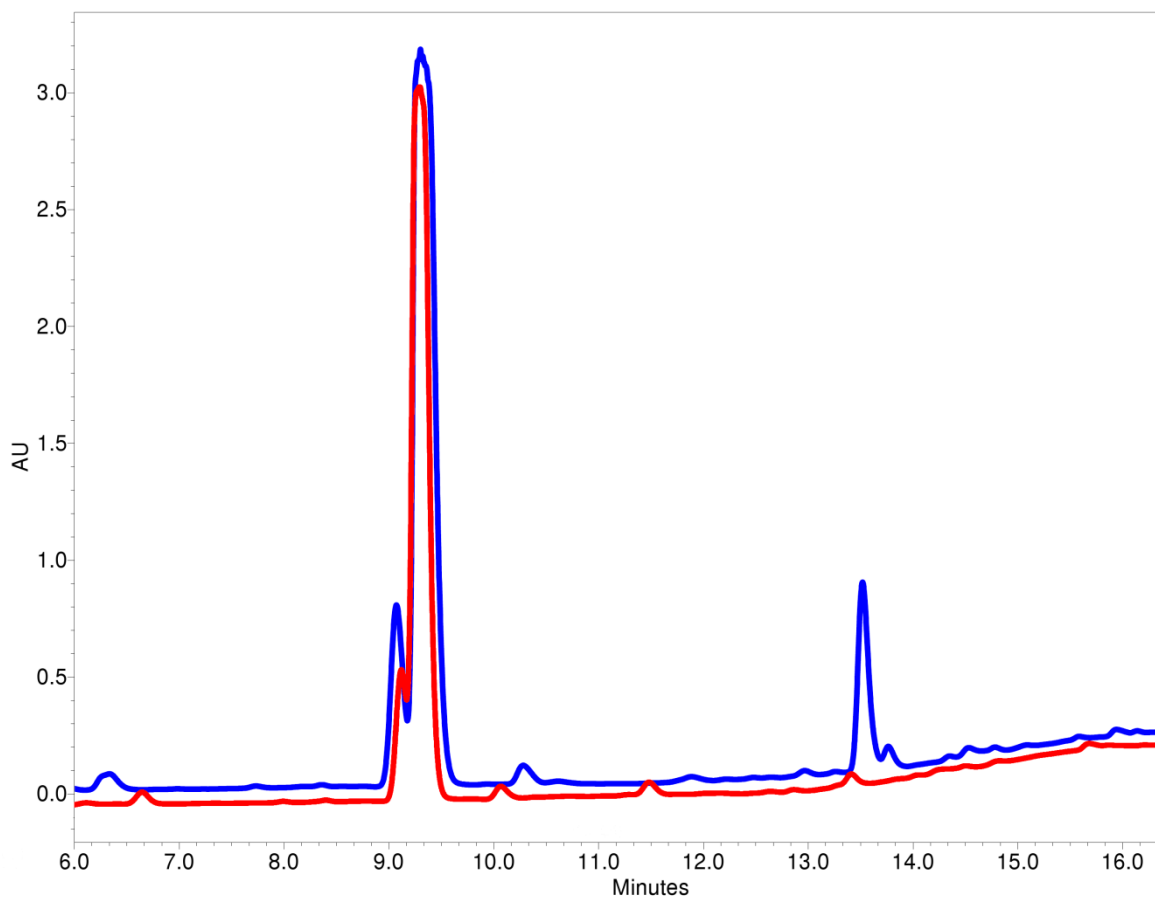


**Figure S18.** Dehydration of (3*R*)-3-hydroxybutanoyl-S-NAC. Reversed-phase HPLC analysis of a control (red, no enzyme) and the RifDH10-catalyzed dehydration (blue) of (3*R*)-3-hydroxybutanoyl-S-NAC (9.2 min), with product eluting at 13.5 min. Product peak was collected and confirmed with LC/MS: expected mass 187.3; observed mass: 187.0.

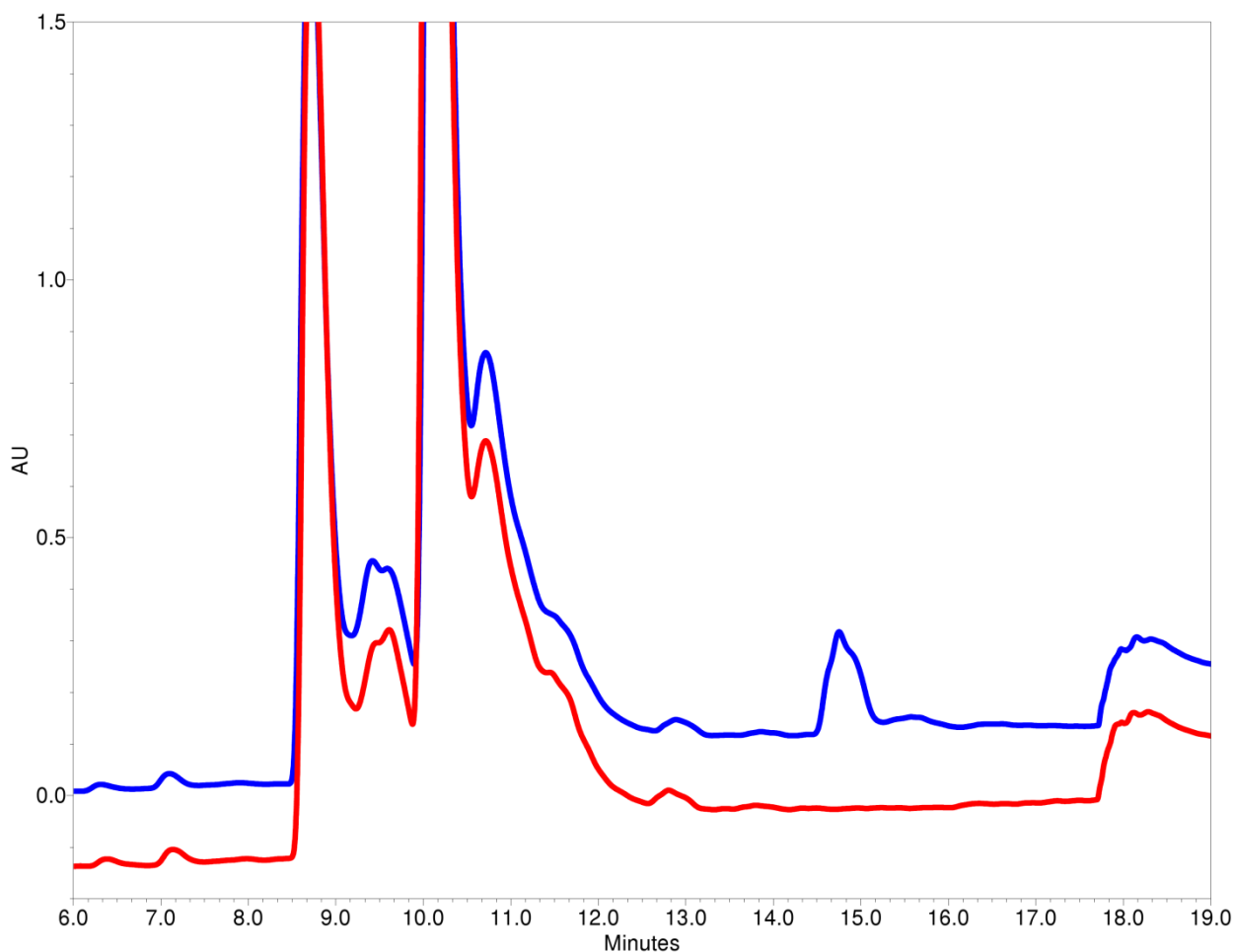


**Figure S19.** Dehydration of (2*R*,3*R*)-2-methyl-3-hydroxypentanoyl-S-NAC. Reversed-phase HPLC analysis of a control (red, no enzyme) and the RifDH10 catalyzed dehydration (blue) of (2*R*,3*R*)-2-methyl-3-hydroxypentanoyl-S-NAC (10.2 min), with product eluting at 14.8 min. The significant peak at 8.9 min is residual (2*RS*)-2-methyl-3-oxopentanoyl-S-NAC which was not reduced by the preceding TyIKR1 catalyzed reduction. Product peak was collected and confirmed with LC/MS: expected mass 215.3; observed mass: 216.0.

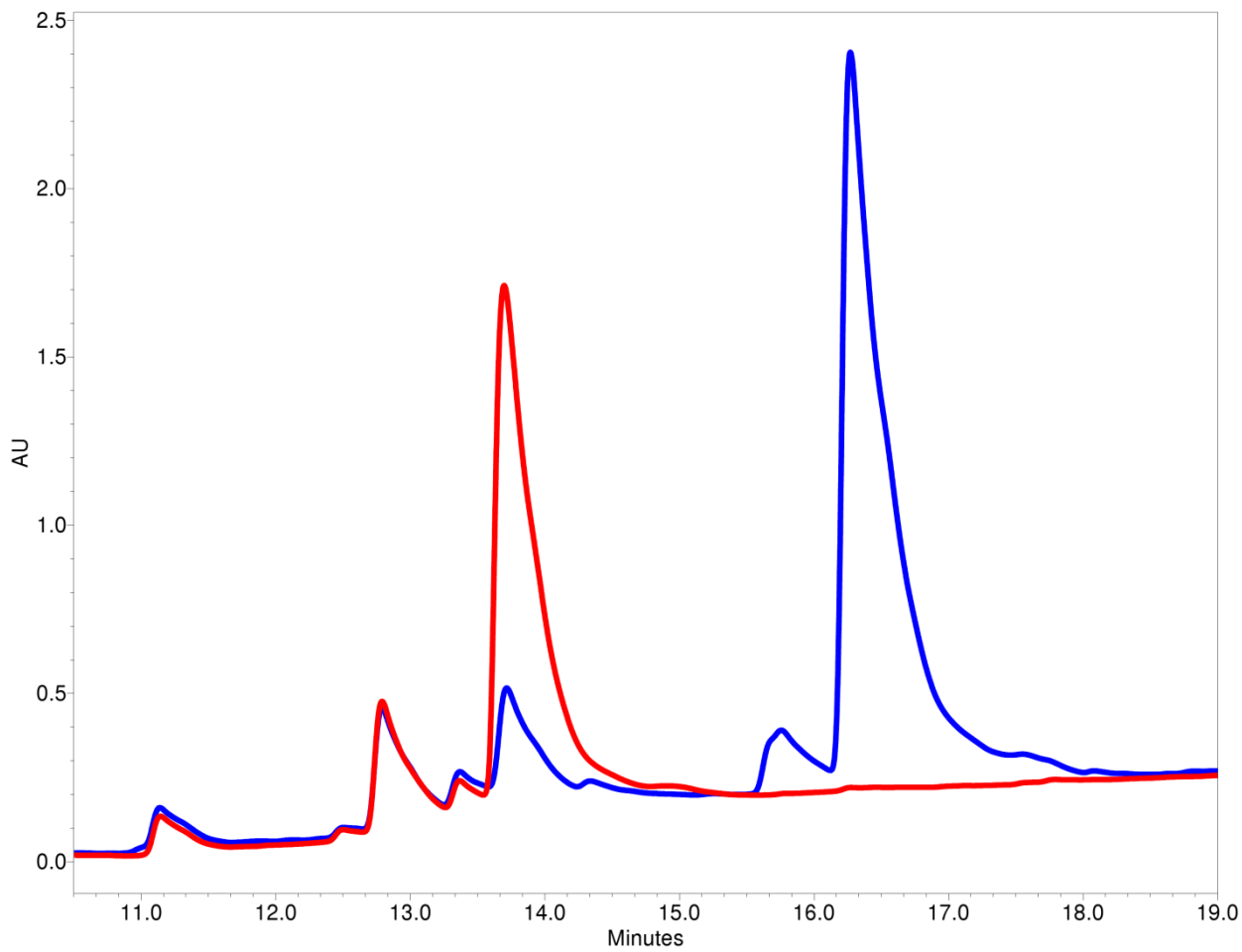


**Figure S20.** Dehydration of (2*R*,3*R*)-2-methyl-3-hydroxypentanoyl-*S*-pantetheine. Reversed-phase HPLC analysis of a control (red, no enzyme) and the RifDH10-catalyzed dehydration (blue) of (2*R*,3*R*)-2-methyl-3-hydroxypentanoyl-*S*-pantetheine (13.8 min), with product eluting at 16.4 min. Product peak was collected and confirmed with LC/MS: expected mass 374.5; observed mass: 374.0.

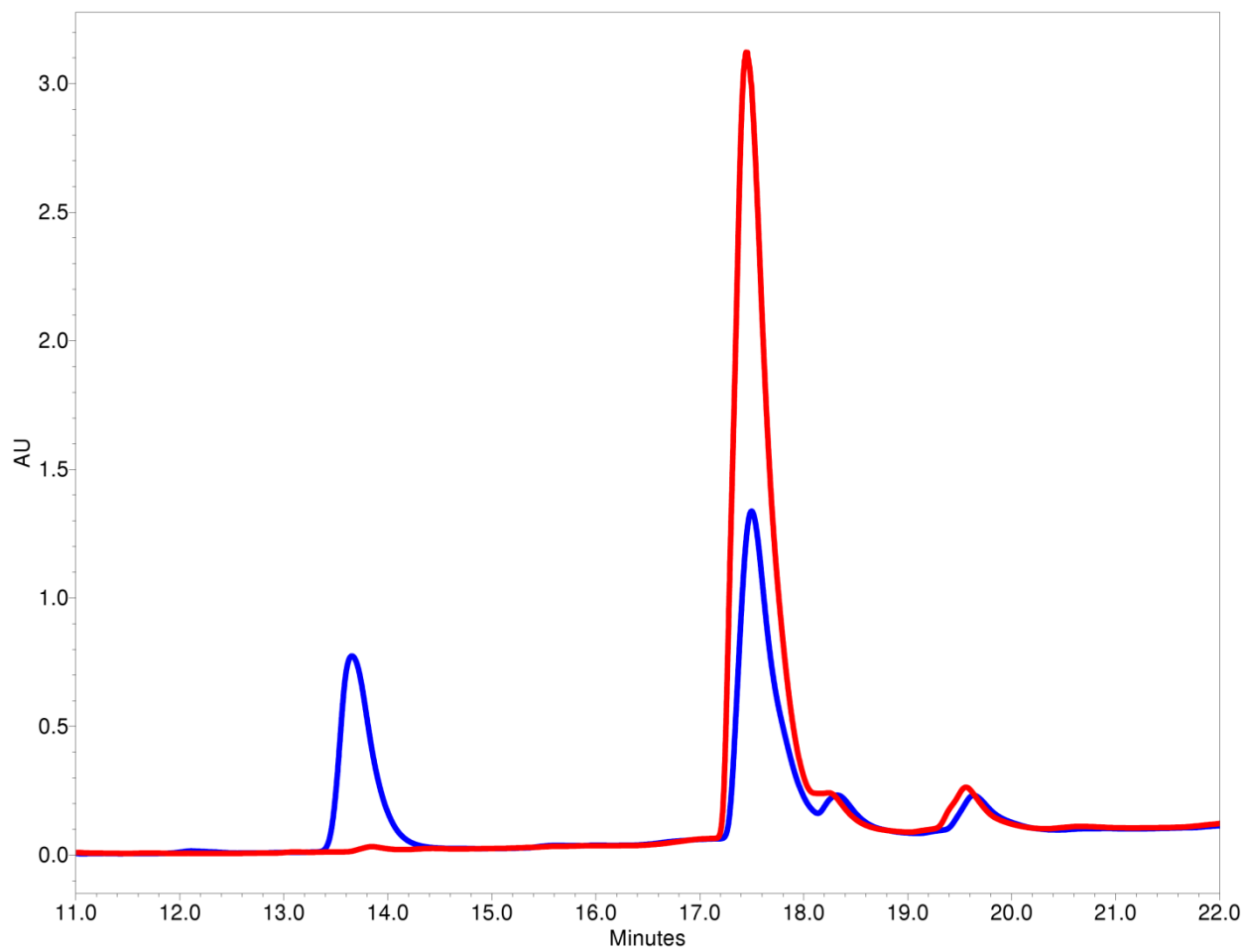


**Figure S21.** Hydration of (*E*)-2-butenoyl-*S*-pantetheine. Reversed-phase HPLC analysis of a control (red, no enzyme) and the RifDH10-catalyzed hydration (blue) of (*E*)-2-butenoyl-*S*-pantetheine (17.6 min), with product eluting at 13.8 min. Product peak was collected and confirmed with LC/MS: expected mass 364.5; observed mass: 365.0.



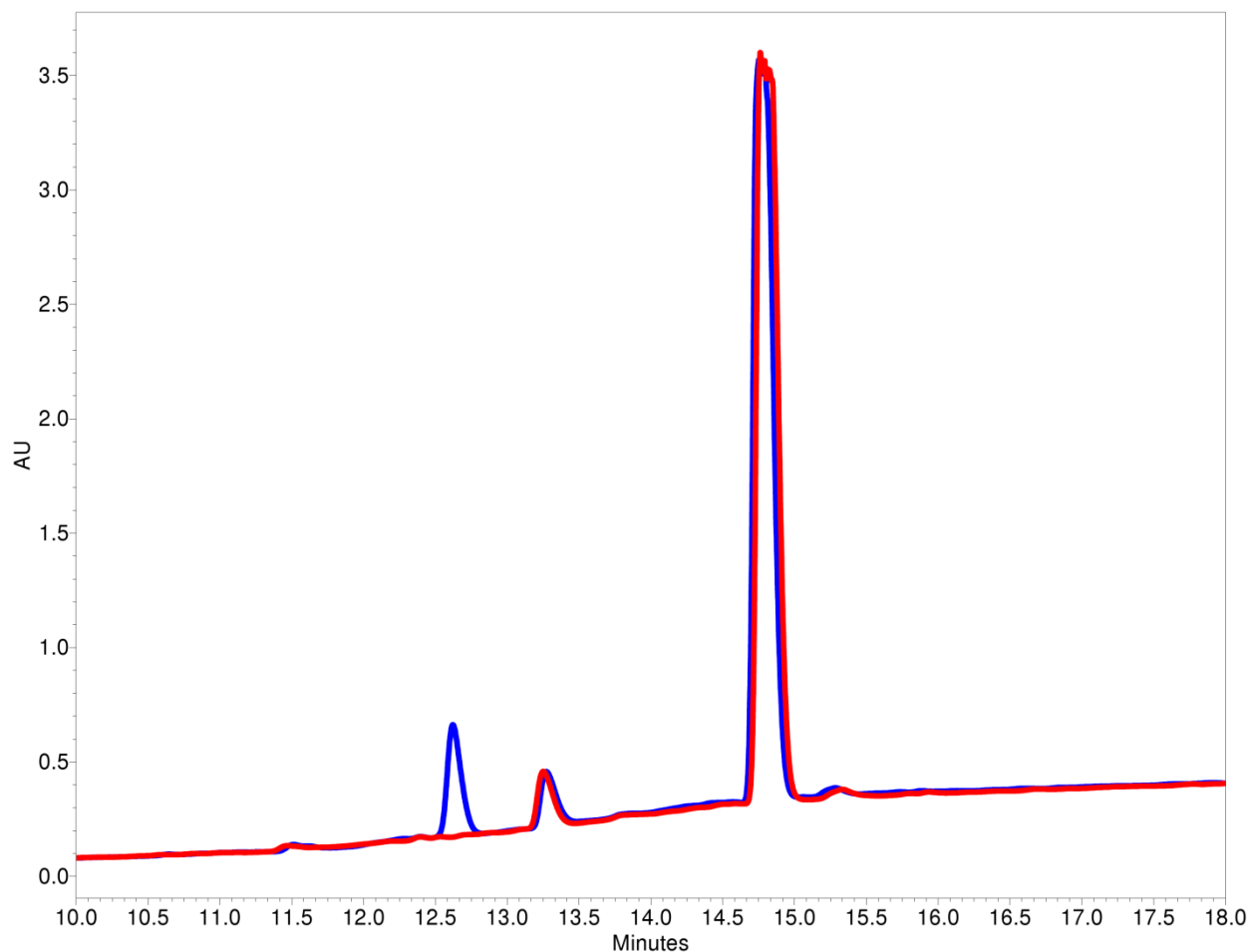


**Figure S22.** Hydration of (*E*)-2-methyl-2-butenoyl-*S*-pantetheine. Reversed-phase HPLC analysis of a control (red, no enzyme) and the RifDH10-catalyzed hydration (blue) of (*E*)-2-methyl-2-butenoyl-*S*-pantetheine (14.8 min), with product eluting at 12.6 min. Product peak was collected and confirmed with LC/MS: expected mass 378.5; observed mass: 378.0.

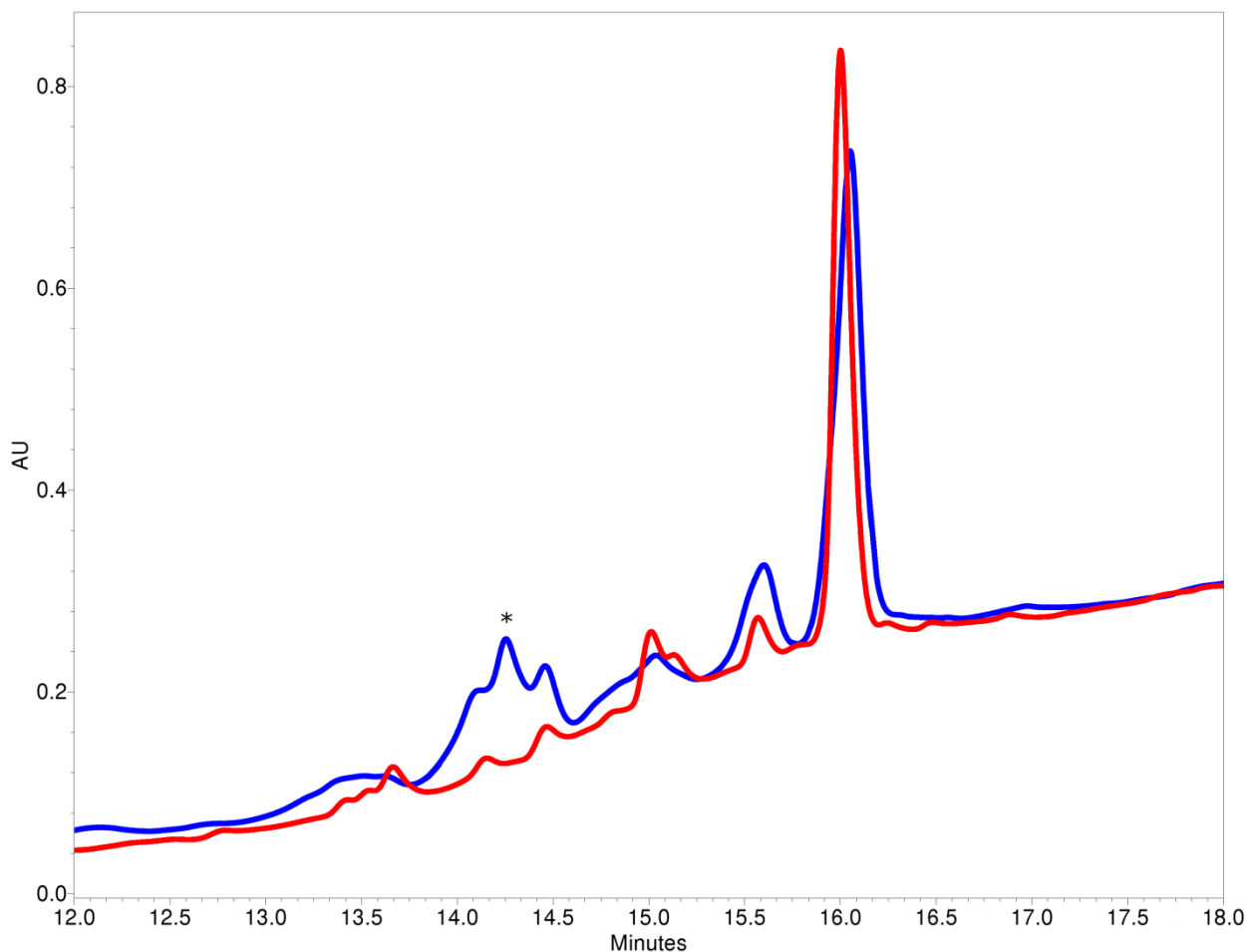


**Figure S23.** Hydration of (*E,E*)-2,4-hexadienoyl-*S*-pantetheine. Reversed-phase HPLC analysis of a control (red, no enzyme) and the RifDH10 catalyzed hydration (blue) of (*E,E*)-2,4-hexadienoyl-*S*-pantetheine (16.1 min), with product eluting at 14.3 min. The hydrated product has been highlighted with an asterisk due to adjacent contaminating peaks, which are also present in the control reaction. Product peak was collected and confirmed with LC/MS: expected mass 390.5; observed mass: 391.0.

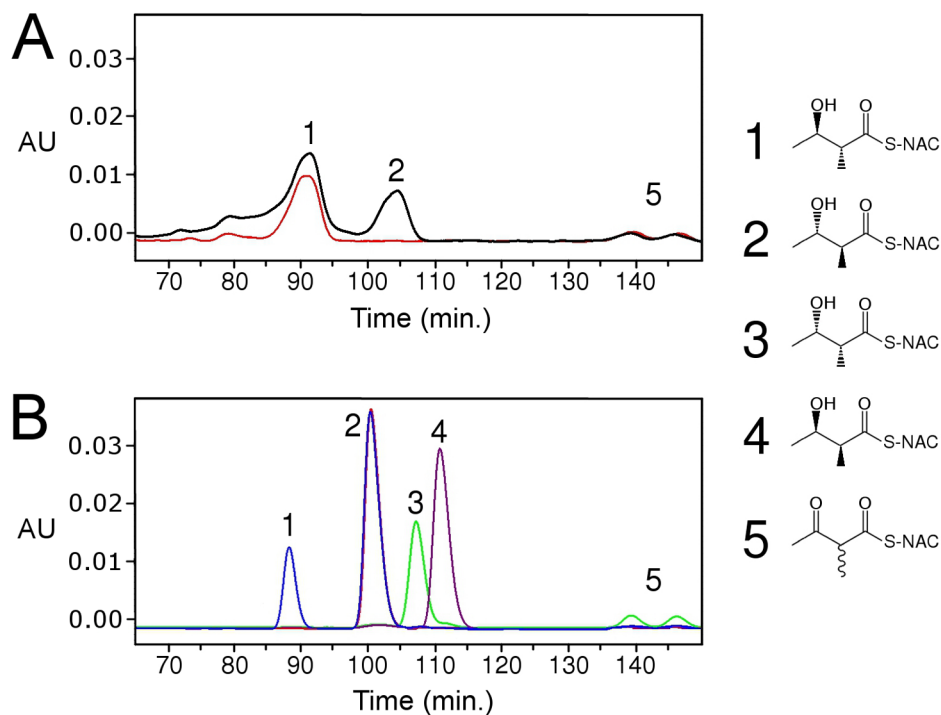


**Figure S24.** Stereochemistry of hydrated product from RifDH10-catalyzed hydration of (*E*)-2-methyl-2-butenoyl-*S*-pantetheine. (*E*)-2-Methyl-2-butenoyl-*S*-pantetheine was incubated with RifDH10, and the resultant hydrated product was purified by reverse-phase HPLC. The acyl group was subsequently transferred to *S*-NAC, and subjected to chiral HPLC analysis. (A) Chiral HPLC trace of the product of the RifDH10 catalyzed hydration of (*E*)-2-methyl-2-butenoyl-*S*-pantetheine (red). The run was repeated after being spiked with authentic (2*S*,3*S*)-2-methyl-3-hydroxybutanoyl-*S*-NAC (black trace). (B) A series of authentic standards analyzed on the same chiral column used to determine retention times of each of the stereoisomers of 2-methyl-3-hydroxybutanoyl-*S*-NAC.

## Supplemental References.

1. Piasecki, S. K., Taylor, C. A., Detelich, J. F., Liu, J., Zheng, J., Komsoukaniants, A., Siegel, D. R., and Keatinge-Clay, A. T. (2011) Employing modular polyketide synthase ketoreductases as biocatalysts in the preparative chemoenzymatic syntheses of diketide chiral building blocks, *Chem. Biol.* 18, 1331-1340.
2. Zheng, J., Gay, D. C., Demeler, B., White, M. A., and Keatinge-Clay, A. T. (2012) Divergence of multimodular polyketide synthases revealed by a didomain structure, *Nat. Chem. Biol.* 8, 615-621.